

# Heat transfer and pressure drop characteristics of yawed fin arrays

A. M. E. ABDEL-LATIF and M. A. SALEH

Mechanical Power Dept., Faculty of Eng., Zagazig University, Zagazig, Egypt

An experimental investigation is carried out to study effects of yaw angle, interfin spacing, and shroud clearance on heat transfer and pressure drop characteristics of square pin fins arranged in staggered and in-line arrays. Measurements were carried out for three values of shroud-to-height ratios  $C/H$ , namely 0.0, 0.5, and 1.0. For each one of these values, measurements were carried out for five values of yaw angles  $\psi$ , namely 0.0, 10, 20, 30, and 45 and three values of Reynolds number ranged from  $3.5 \times 10^3$  -  $1.1 \times 10^4$ . The spanwise spacing  $S_z$  was varied from 10 to 80 mm while the normal to span spacing  $S_x$  was varied from 18 to 80 mm. Experiments were performed with air as the working fluid. It is found that the heat transfer rate increases gradually with increasing yaw angle reaching a maximum at  $\psi = 30$  before it decreases with further increase in  $\psi$ . Also it is found that the optimum interfin spacing in both spanwise  $S_z$  and normal to span  $S_x$  directions is 2.0 b, and 1.8 b, respectively (where b is the side length of pin fin cross-section) regardless of yaw angle, shroud clearance, and type of array used. A general heat transfer and friction correlations have been developed taking into account spanwise spacing  $S_z$ , normal to span spacing  $S_x$ , yaw angle  $\psi$ , shroud-to-height ratio  $C/H$ , and flow Reynolds number  $Re$  for both in-line and staggered arrangements.

تناقش الدراسة تأثير زاوية ميل الزعانف على اتجاه السريان والمسافات الطولية والعرضية بين الزعانف وكذلك مسافة الخلووص بين غطاء أفقى وأعلى نقطة على الزعانف على انتقال الحرارة وانخفاض الضغط لمصفوفات من الزعانف فى تتابع خطى وكذلك

متداخل. وقد أجريت التجارب لثلاث قيم لنسبة الخلووص الى ارتفاع الزعانف (خ/ع) وهى صفر، ٠.٥، ١.٠. وقد تمت القياسات لزاوية ميل الزعانف على اتجاه السريان وهى صفر، ١٠، ٢٠، ٣٠، ٤٥ وكذلك لثلاث قيم من رقم رينولدز تتراوح بين  $3.5 \times 10^3$  -  $1.1 \times 10^4$  لكل قيمة من نسبة الخلووص الى الارتفاع (ع/خ). وكانت المسافة بين الزعانف فى اتجاه السريان

تتراوح بين ١٠ - ٨٠ مم بينما كانت المسافة بين الزعانف فى الاتجاه العمودى على السريان تتراوح بين ١٨ - ٨٠ مم. وقد وجد ان معدل انتقال الحرارة يتزايد تدريجيا مع زيادة زاوية ميل الزعانف على اتجاه السريان ليصل الى اعلى قيمة عند زاوية مقدارها ٣٠ ثم يتناقص مع اى زيادة اخرى فى زاوية الميل. ايضا بينت التجارب ان احسن مسافة لانتقال الحرارة بين الزعانف فى اتجاه السريان والاتجاه العمودى على السريان هى ٢ب، ١.٨ب على الترتيب حيث ب هو طول جانب الزعنفة. وقد تم استنتاج معادلات عامه لانتقال الحرارة والاحتكاك تربط كل المتغيرات الوارد ذكرها.

**Keywords:** Square pin fin, Yaw angle, In-line and staggered arrangements.

## 1. Introduction

Augmentation of heat transfer from engineering components has attracted the attention of researchers for many years. The development of very powerful gas turbine engines for military aeroplanes required the development of a very efficient technique for cooling turbine blades. One way of doing this is through the application of forced convection to fin array configuration inside the blade. Another area where heat transfer

augmentation is required is the micro miniaturization of electronic components for digital computers and the instrumentation of modern aircrafts.

The subject of heat transfer in arrays of rectangular blocks, especially for the periodic fully developed flow, has been studied by many investigators. Sparrow et al. [1,2] have reported heat transfer and pressure drop in arrays of rectangular blocks with barriers and missing blocks. They used a mass transfer technique with the heat-mass analogy to

obtain the so-called adiabatic heat transfer coefficient. The object of their work was to study the effect of the missing block and barriers on thermal-hydraulic behavior of the array. Molki et al. [3] investigated the heat transfer in the entrance region of an in-line array of heated blocks. The focus of their work was on the entrance heat transfer coefficients and the associated thermal wake effects.

Sparrow and Samie [4] experimentally investigated the heat transfer and pressure drop from one and two arrays of tubes in a Reynolds number range from 7500 to 32,000. They found that when one row of tubes was used, both Nusselt number and pressure drop were very sensitive to the pitch distance in the spanwise direction (pitch distance between tubes). Similar trends were obtained for a staggered two-row array of finned tubes. Metzger et al. [5] reported measurements of heat transfer associated with staggered arrays of short circular pin fins (length-to-diameter ratio of 1). The staggered array arrangements considered were those encountered in cooled gas turbine engine airfoils. Measurements were conducted over a Reynolds number range of  $10^3$  to  $10^5$ . They found that, in general, the Nusselt number increases for the first three rows and then it declines for the remaining ones.

In a series of experimental investigations, Moffat et al. [6-14] have extensively studied various aspects of thermal-hydraulic behavior of the arrays of electronic components. The overall objective of their effort was to develop techniques and data base needed to predict the operating temperature of the blocks. They have also emphasized the very crucial point that the adiabatic heat transfer coefficient, which is reported in the electronics cooling literature, should be used in reference to the adiabatic fluid temperature.

Several investigators [15-24] have attempted to increase heat transfer in pin-finned plate exposed to an impinging air stream. The pin fins are aligned with the air approach velocity. The overall objectives of their effort were to select the optimal spacings between electronic components (e.g. boards) and fin-to-fin spacing. They also constructed a numerical model and generated a considerable

volume of optimal-spacing and maximum heat transfer data, for various combinations of flow condition (Re), pin dimensions (b/L, H/L), and fluid type (Pr). A numerical simulation of three dimensional flow and temperature field was performed by Sathe et al. [23] in a study of heat sinks with square pin fins, in which the spacing was fixed. The thermal performance of complete sink and fan assembly was simulated using a commercial computational package by Kamath [17]. Three geometries with fixed fin spacings were considered: square pin fins, straight fins and radial fins. Related advances were also made in the area of liquid jet impingement cooling. Sullivan et al. [25] conducted experiments with three heat sink geometries with square pin fins, in which two fin spacings were tested. Heindel et al. [26] reported data for one heat sink with radial fins.

Tahat [27] conducted an experimental investigation on the optimization of pin-fin arrays subjected to forced convective heat transfer. Heat transfer as well as pressure drop were measured for in-line and staggered arrays with zero gap clearance ratio. Jubran et al. [28] investigated the effect of the interfin spacing and missing pin on the heat transfer from cylindrical pin fins arranged in staggered and in-line arrays. They found that the staggered arrangement of the array tends to give higher heat transfer than that of the in-line ones. The effect of missing pin on in-line and staggered arrays with various interfin spacing is negligible but staggered arrays are most sensitive to the missing pin with a 7 percent reduction in the heat transfer.

It is anticipated that yawing fin arrays to flow direction will have a pronounced effect on both heat transfer and pressure drop characteristics of these arrays. To the knowledge of the present authors the case of yawed fin arrays to flow direction has not been dealt with before. In the present work, the effect of yaw angle on heat transfer rates and friction factor is investigated for both in-line and staggered arrays of square pins. A wide range of interfin spacing is considered and more general correlations are obtained. The present work also aims to make optimization of the pin fin array configuration at various flow conditions.

## 2. Experimental setup and test procedure

The experiments were performed in an open type wind tunnel which has a square test section  $440\text{ mm} \times 440\text{ mm}$ , and  $1000\text{ mm}$  length with maximum air speed of  $23\text{ m/s}$ . Fig. 1 shows the general arrangement of the fin array in the test section. The side walls of the test section are made from Plexiglass. The middle bottom side of the test section has a rectangular slot ( $210\text{ mm} \times 195\text{ mm}$ ) to accommodate the light metal alloy base of the square pin fin array. Five slots with different yaw angles were made in the bottom of the test section. A container box is attached to the slot to enclose the aluminum base. This box was filled with insulating material to minimize heat dissipation to atmosphere as shown in fig. 1. The air flow is adjusted by a gate valve.

The square pin fin array is composed of a  $210\text{ mm} \times 195\text{ mm}$  horizontal rectangular base with a thickness of  $30\text{ mm}$ . Square pin fins of  $10\text{ mm}$  in side,  $60\text{ mm}$  in height are mounted on and protruding vertically upward from the rectangular base. Both the base and the fins are made of high-thermal-conductivity aluminum alloy. A thin layer of thermally conducting epoxy cement (electrically insulated) serves to ensure good contact between the rectangular base and pin fins. The number of pin fins can be adjusted to suit the required spacing between the fins in the spanwise ( $z$  axis) direction and in the normal direction ( $x$  axis). The interfin spacing in the spanwise direction (distance between two adjacent fins) is varied from  $10\text{ mm}$  to  $80\text{ mm}$ , and in the normal-to-span direction from  $18\text{ mm}$  to  $80\text{ mm}$ . Nichrome wire uniformly and closely wound on a mica sheet is used for heating the rectangular base and was firmly attached to the bottom of the base by a set of screws. A guard heater is used to minimize the heat losses to the outside surroundings. A guard heater is separated from the main heater by a copper sheet ( $3\text{ mm}$  thick). Two asbestos sheets ( $6\text{ mm}$  thick) and copper sheet ( $3\text{ mm}$  thick) are fixed below the guard heater. The enclosure is filled with glass wool insulating material as shown in fig. 2-a. The electric power input to the main plate heater and the guard heater are controlled by an auto-transformer (variac), and are measured by a wattmeter with an accuracy  $\pm 1.5\%$  of

readings. The pin fin array is kept at constant uniform temperature of  $50 \pm 0.5\text{ C}$ . Figs 2-b and 2-c show a description of shroud pin fin array geometry and air stream flow. The top cover (shroud) is adjustable to give different shroud clearance spaces over the fin tips.

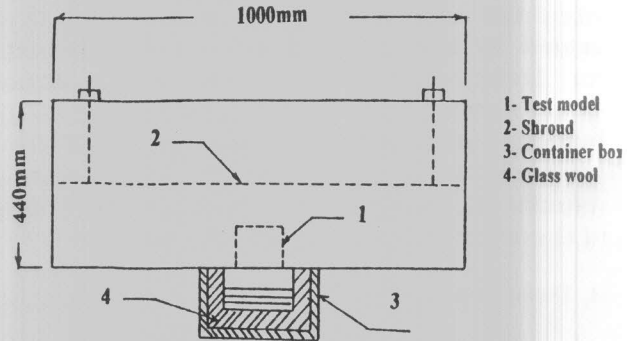


Fig. 1. Schematic diagram of test section.

The steady-state temperature of the rectangular base of the fin array was measured by ten copper-constantan thermocouples distributed uniformly over the base and embedded  $15\text{ mm}$  deep from the surface of the base plate. The readings of these thermocouples were recorded using a digital thermometer with resolution of  $\pm 0.5\text{ C}$  and the average of the steady state readings of these thermocouples are taken as the temperature of the base plate. The inlet temperature of the air stream is taken as the average reading of five copper-constantan thermocouples located uniformly at the inlet of the test section (distributed in three rows,  $14.7\text{ cm}$  distance between them. Two thermocouples in the upper and lower rows,  $14.7\text{ cm}$  distance between thermocouples in each row. One thermocouple in the center of the middle row). Similarly, the outlet temperature of the air stream is taken as the average reading of five copper-constantan thermocouples located uniformly at the outlet of the test section. The pressure drop across the pin fin array is measured using two static pressure tapings in the surface of the cover plate (shroud) just over the pin fin array. These tapings are connected to a micromanometer of resolution of  $\pm 0.01\text{ mm H}_2\text{O}$ .

Before the start of a run, the number of pin fins is adjusted to the required spacing

between the fins in the spanwise and normal-to-spanwise directions. The clearance gap between the fin tip and the horizontal shroud is adjusted for a predetermined gap. The base plate with the pin fins on it are fixed at the desired yaw angle. Then, to prevent air leakage from the test section, all suspected joints are sealed by silicon rubber and thoroughly tested for leaks with the aid of soap solution. Subsequently, the flow and power to the heaters are turned on and adjusted for a predetermined flow rate. A steady state is usually achieved after three hours (no change of thermocouples reading with time).

### 3. Data reduction

The friction factor of the periodic fully developed flow is calculated from the pressure drop across the test duct and the mean velocity of the air and is expressed as:

$$f = [(-\Delta p / \Delta X) \cdot D_c] / (\rho \cdot U^2 / 2), \quad (1)$$

where the pressure gradient,  $\Delta p / \Delta X$ , is evaluated by taking the ratio of the pressure difference and the distance of the two pressure taps. In the present investigation, the friction factor is obtained under isothermal conditions (tests without heating). The maximum uncertainty in (f) is estimated to be less than 7.3 percent for Reynolds number greater than 10,000 using the uncertainty estimation method of Kline and McClintock [29].

The convective heat transfer coefficient is evaluated from,

$$h = Q_{conv} / [A_b \{T_b - (T_{in} + T_{out} / 2)\}], \quad (2)$$

where  $A_b$  is the total heat transfer area given by

$$A_b = w L + (4 b H N_{fz} N_{fx}),$$

and

$$Q_{conv} = Q - Q_{loss}. \quad (3)$$

Where  $Q_{conv}$  represents the net heat transfer rate from the fins to the coolant, and is calculated by subtracting the heat loss ( $Q_{loss}$ ) from the supplied electrical power (Q). The

heat loss can be estimated by the following equation:

$$Q_{loss} = Q_a + Q_{rad}. \quad (4)$$

The radiative heat loss from a duralum plate fin assembly,  $Q_{rad}$ , was evaluated by Naik et al. [30] for a similar setup to be about 0.5 percent of the total heat input.  $Q_a$  is the conductive heat loss from the sides of the heated rectangular base, and is estimated to be less than 1.5 percent of the total electric power input. Tahat [27] conducted similar experimental tests, and reported that the total heat losses from the pin fin array, with the radiative heat transfer losses being included, were only 2.5 percent of the total heat input. Using these findings, one could assume with some confidence that  $Q_{loss}$  may be ignored. Then eq. (3) reduces to:

$$Q_{conv} = Q.$$

The total net heat transfer rate from the test duct to the cooling air is further checked with the cooling air enthalpy rise along the test duct. A satisfactory agreement is achieved, which confirms good energy conservation in the experiments.

Reynolds number (Re) and Nusselt number (Nu) may be written as:

$$Re = G_{max} b / \mu_{air}. \quad (5)$$

$$Nu = h b / k_{air}. \quad (6)$$

where;

$$G_{max} = m / A_{fr}.$$

Using the method of Kline and McClintock [29], the maximum uncertainty of the Nusselt number is less than 6.2 percent for Reynolds number greater than 10,000.

### 4. Results and discussion

Experiments were carried out to investigate the effect of yaw angle, shroud-to-height ratio, interfin spacing, and mass flow rate on heat transfer and pressure drop characteristics of square fin arrays arranged in in-line, and staggered. Measurements were

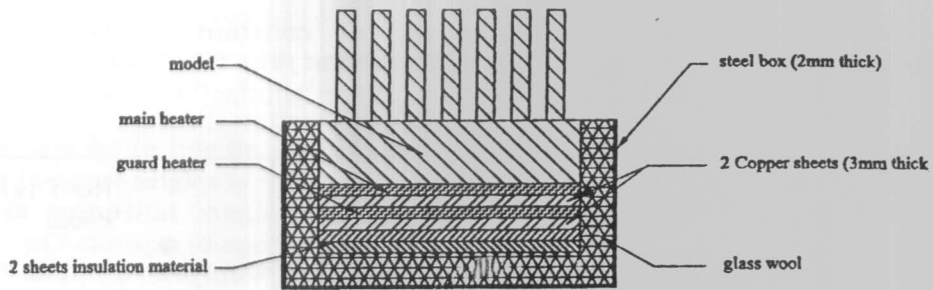


Fig. 2-a. Assembly of test model.

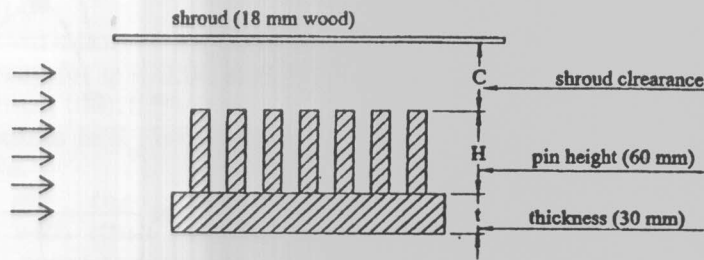


Fig. 2-b. Description of shrouded square fin array.

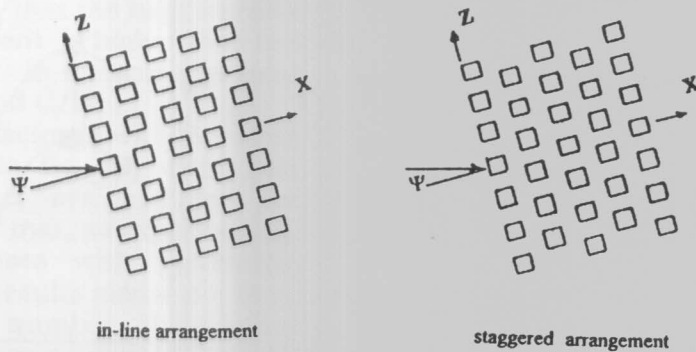


Fig. 2-c. Description of pin geometry and air stream flow.

carried out for three values of shroud-to-height ratios  $C/H$ , namely 0.0, 0.5, and 1.0. For each one of these values, measurements were carried out for five values of yaw angle  $\psi$ , namely  $0.0^\circ$ ,  $10^\circ$ ,  $20^\circ$ ,  $30^\circ$ , and  $45^\circ$  and three values of Reynolds number ranged from  $3.5 \times 10^3$ ,  $6.7 \times 10^3$  and  $1.1 \times 10^4$ . The spanwise spacing  $S_z$  was varied from 10 to 80 mm while the normal-to-span spacing  $S_x$  was varied from 18 to 80 mm.

Effect of yaw angle on Nusselt number at different values of  $C/H$  and two values of  $S_z$  for in-line arrangement ( $S_x=18$  mm,  $Re=1.1 \times 10^4$ ) is shown in fig. 3.

It is seen that Nusselt number increases gradually with increasing yaw angle reaching a maximum at  $\psi = 30^\circ$  then it decreases with

further increase in  $\psi$ . This may be attributed to the existence of a strong flow separation zone at  $\psi = 30^\circ$  on the first row of blocks of the array. This flow separation has an enhancing effect on the blocks-averaged heat transfer coefficient. Fig. 3 also shows that  $Nu$  at  $\psi = 45^\circ$  is lower than that at  $\psi = 30^\circ$ . At  $\psi = 45^\circ$  the flow over pin fins is a wedge flow and there is no separation at the leading edge of the pins. Also the figure shows that for  $10^\circ < \psi \leq 45^\circ$  values of  $Nu$  are greater than these for  $\psi = 0.0^\circ$ . It is also seen that  $Nu$  for the array with  $S_z=20$  mm is greater than the corresponding  $Nu$  for  $S_z=55$  mm. Fig. 4 shows variation of Nusselt number  $Nu$  with spanwise spacing ratio  $S_z/b$  at different shroud-to-

height ratios  $C/H$  and different Reynolds numbers  $Re$  at normal-to-span spacing  $S_x = 18$  mm and yaw angle  $\psi = 0.0$  for in-line arrangement. It is seen that the optimum interfin spacing in the spanwise direction, which corresponds to maximum  $Nu$  is  $S_z/b = 2.0$  for all shroud-to-height ratios  $C/H$  and Reynolds numbers  $Re$ . Fig. 4 also shows that  $Nu$  increases with decreasing  $C/H$ . This may be attributed to the fact that as the clearance above the fins is increased, the flow resistance

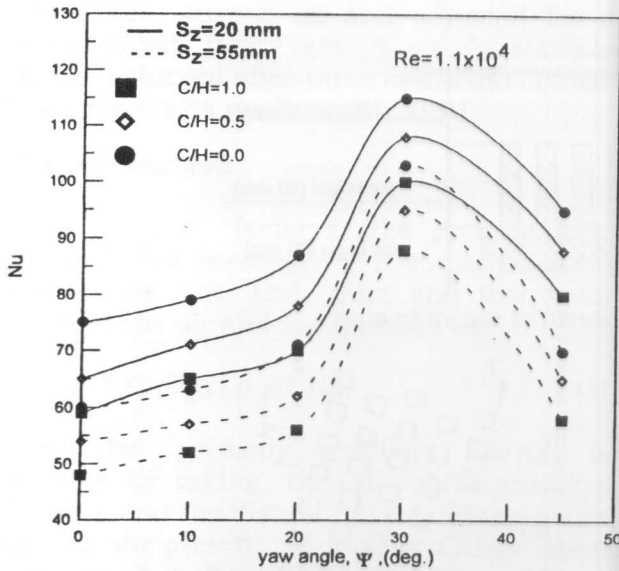


Fig. 3. Effect of yaw angle on Nusselt number for in-line arrangement ( $S_x = 18$ mm,  $Re = 1.1 \times 10^4$ ).

of the alternative path diminishes relative to that of the entire fin spacing, so that the highest velocities occur in the clearance gap. It can also be seen that  $Nu$  decreases, after reaching the maximum value at  $S_z/b = 2$  for further increase in  $S_z/b$ . This is due to the fact that as  $S_z/b$  increases the number of fins in the spanwise direction decreases and hence the heat transfer decreases. A similar observation was reported by ref. [28] for cylindrical pin fin arrays at  $\psi = 0.0$ ,  $C/H = 0.0$  and  $Re = 3.7 \times 10^4$ . Results of ref. [28] are plotted in fig. 4. Fig. 4 also shows that  $Nu$  increases with increasing  $Re$ .

Figs. 5 and 6 show variation of Nusselt number with spanwise spacing ratio  $S_z/b$  for  $\psi = 30$  and  $45$  respectively. These figures are presented for in-line fin array for different shroud-to-height ratios  $C/H$  and different  $Re$

at constant normal-to-span spacing  $S_x = 18$  mm. The family of curves seen in figs. 5 and 6 are similar to those observed in fig. 4 for  $\psi = 0.0$ .

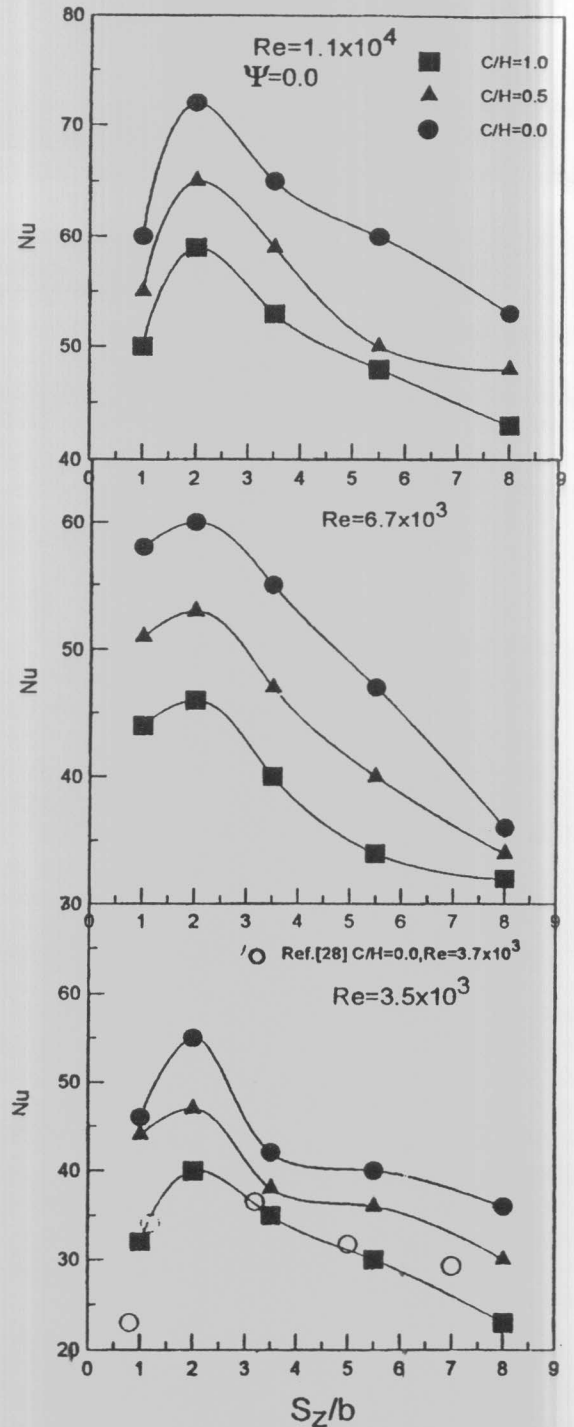


Fig. 4. Variation of Nusselt number with spanwise spacing ratio  $S_z/b$  for in-line fin array ( $\psi = 0.0, S_x = 18$  mm).

Variation of Nusselt number with normal-to-span spacing ratio  $S_x/b$  for different shroud-to-height ratios is shown in figs. 7 and 8. These figures are for in-line fin array with  $S_z=20$  mm, and two yaw angles  $\psi = 0.0^\circ, 30^\circ$ , respectively. It is seen that maximum heat transfer occurs at normal-to-span spacing  $S_x/b=1.8$  for all shroud clearance and flow rates. Also it is seen that Nusselt number increases with increasing Re. Figs. 7 and 8 also show that values of  $Nu$  at  $\psi = 30^\circ$  are greater than those for  $\psi = 0.0^\circ$ .

Figs. 9 and 10 show variation of  $Nu_0$  with  $S_z/b$  for staggered fin array for  $\psi = 0.0^\circ$  and  $30^\circ$ , respectively. The optimum interfin spacing for this case again corresponds to  $S_z/b=2.0$  for all values of  $C/H, \psi$ , and Re.

The performance of the in-line arrangements compared with that of the staggered one under the same experimental conditions is shown in figs. 11 and 12. These figures indicate clearly that the heat transfer for staggered arrangement is higher than the corresponding one for in-line arrangement regardless of  $S_z/b, \psi$ , and  $C/H$ .

Variation of friction factor ( $f$ ) with Reynolds number is depicted in fig. 13, where the results of smooth duct are included for comparison. It is seen that, as expected, the friction factor decreases with increasing Reynolds number. The results also show that, for a given Reynolds number, the friction factor decreases with increasing  $C/H$ . Fig. 13 reveals that ( $f$ ) for finned duct is 3-9 times greater in magnitude than that of a smooth duct. The results also show that the staggered fin arrays have a friction factor greater than that for in-line fin arrays, and the friction factor increases with increasing yaw angle.

Nusselt number  $Nu$ , Reynolds number  $Re$ , spanwise spacing  $S_z$ , normal-to-span spacing  $S_x$ , and yaw angle  $\psi$  were correlated using the following form:

$$Nu = a (Re)^b (S_z/w)^c (S_x/L)^d (\cos \psi)^e, \quad (7)$$

where  $a, b, c, d$ , and  $e$  are arbitrary constants. The following correlations were obtained<sub>3</sub> for Reynolds number ranged from  $3.5 \times 10^3$  to  $1.1 \times 10^4$ , spanwise spacing  $S_z$  ranged from 10 to 80 mm, normal-to-span spacing  $S_x$  ranged from 18 to 80 mm, and yaw angle  $\psi$  ranged from 0.0 to 30.

A least-squares fit to the data yields the following correlations.

For  $C/H = 0.0$ :

*in-line arrangement,*

$$Nu = 2.24 (Re)^{0.242} (S_z/w)^{-0.215} (S_x/L)^{-0.32} (\cos \psi)^{-3.01}, \quad (8)$$

with a spread of  $\pm 11\%$ ,

*staggered arrangement,*

$$Nu = 6.66 (Re)^{0.19} (S_z/w)^{-0.127} (S_x/L)^{-0.24} (\cos \psi)^{-2.15}, \quad (9)$$

with a spread of  $\pm 12.5\%$ .

For  $C/H = 0.5$ :

*in-line arrangement,*

$$Nu = 1.29 (Re)^{0.28} (S_z/w)^{-0.228} (S_x/L)^{-0.344} (\cos \psi)^{-3.3}, \quad (10)$$

with a spread of  $\pm 10.5\%$ ,

*staggered arrangement,*

$$Nu = 3.38 (Re)^{0.24} (S_z/w)^{-0.149} (S_x/L)^{-0.266} (\cos \psi)^{-2.65}, \quad (11)$$

with a spread of  $\pm 11.5\%$ .

Finally, for  $C/H=1.0$ :

*in-line arrangement,*

$$Nu = 1.05 (Re)^{0.288} (S_z/w)^{-0.236} (S_x/L)^{-0.356} (\cos \psi)^{-3.41}, \quad (12)$$

with a spread of  $\pm 9.7\%$ ,

*staggered arrangement,*

$$Nu = 0.38 (Re)^{0.46} (S_z/w)^{-0.156} (S_x/L)^{-0.28} (\cos \psi)^{-2.78}, \quad (13)$$

with a spread of  $\pm 14\%$ .

Reynolds number ( $3.5 \times 10^3 \leq Re \leq 1.1 \times 10^4$ ), shroud-to-height ratio ( $0.0 < C/H \leq 1.0$ ), yaw angle ( $0.0 \leq \psi \leq 30^\circ$ ) and friction factor  $f$  can be correlated as follows:

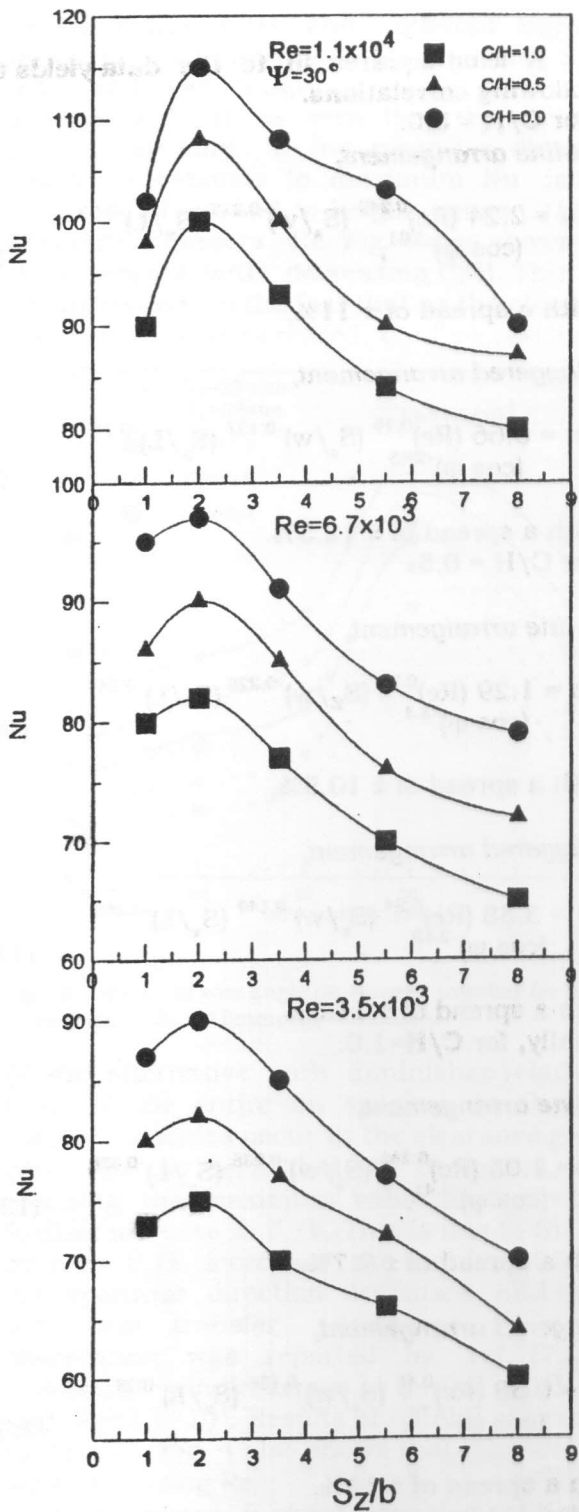


Fig. 5. Variation of Nusselt number with spanwise spacing ratio,  $S_z/b$  for in-line fin array ( $\Psi=30^\circ, S_x=18\text{mm}$ ).

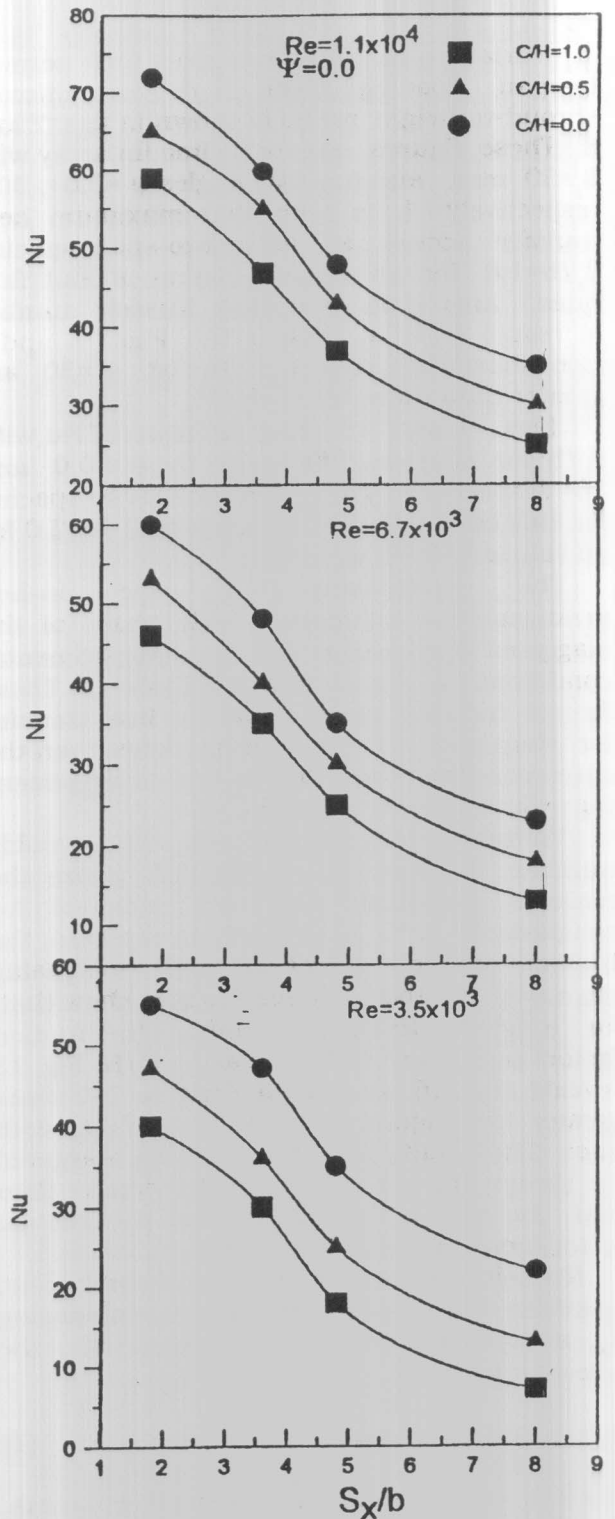


Fig. 6. Variation of Nusselt number with spanwise spacing ratio,  $S_z/b$  for in-line fin array ( $\Psi=45^\circ, S_x=18\text{mm}$ ).



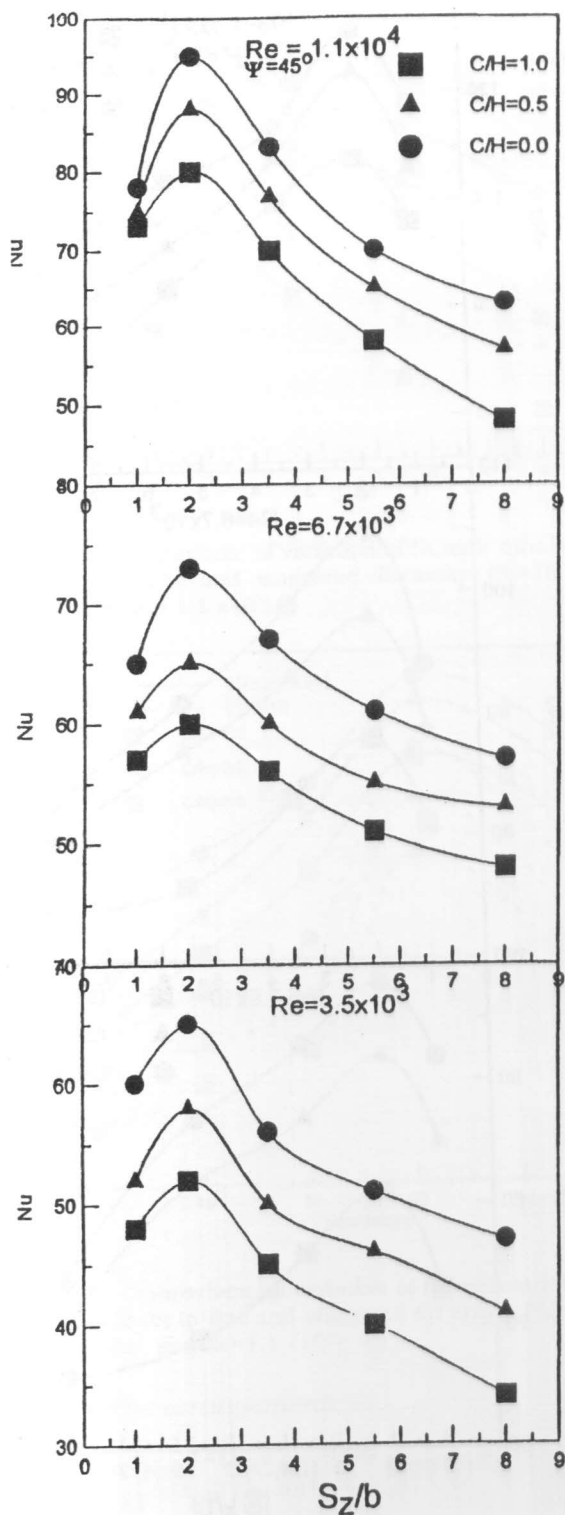


Fig.7. Variation of Nusselt number with normal-to-span spacing ratio,  $S_x/b$  for in-line array ( $\psi=0.0$ ,  $S_z=20\text{mm}$ ).

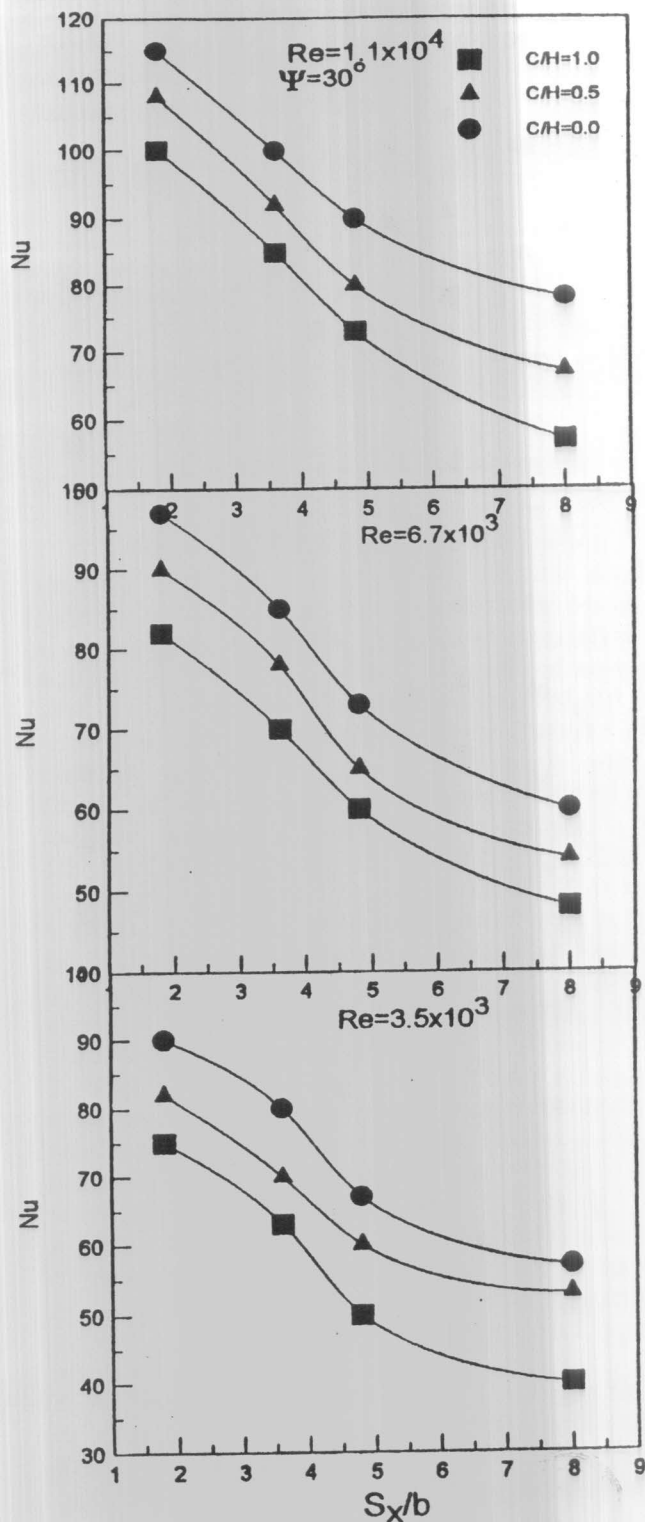


Fig. 8. Variation of Nusselt number with normal-to-span spacing ratio,  $S_x/b$  for in-line fin array ( $\psi=30^\circ$ ,  $S_z=20\text{mm}$ ).

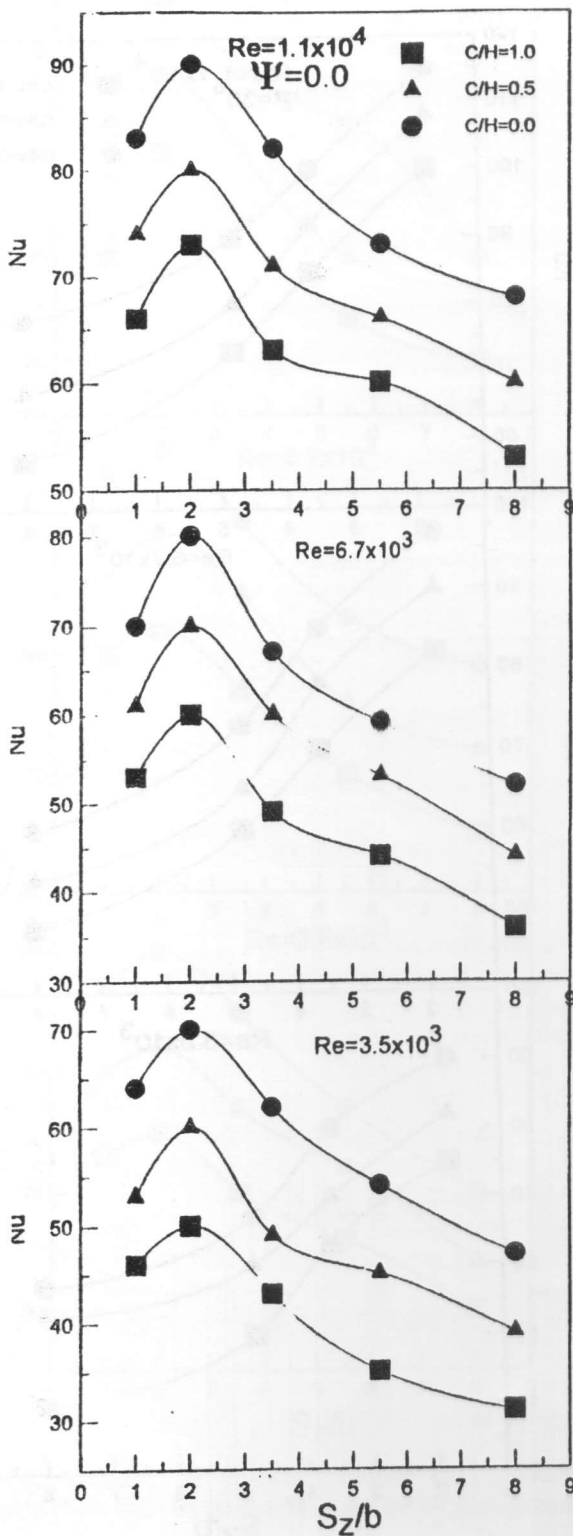


Fig. 9. Variation of Nusselt number with spanwise spacing ratio,  $S_z/b$  for staggered shroud fin array ( $S_x=18\text{mm}$ , and  $\psi=0.0$ ).

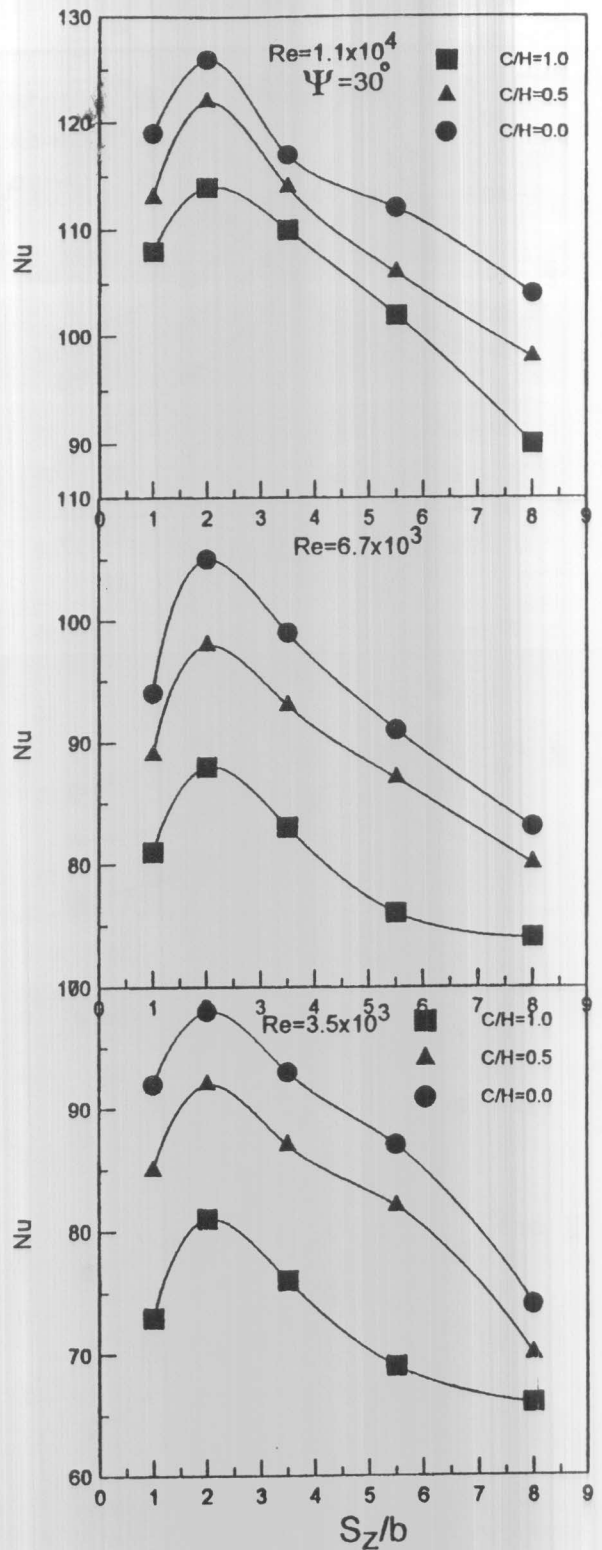


Fig. 10. Variation of Nusselt number with spanwise spacing ratio,  $S_z/b$  for staggered shroud fin array ( $S_x=18\text{mm}$ ,  $\psi=30^\circ$ ).

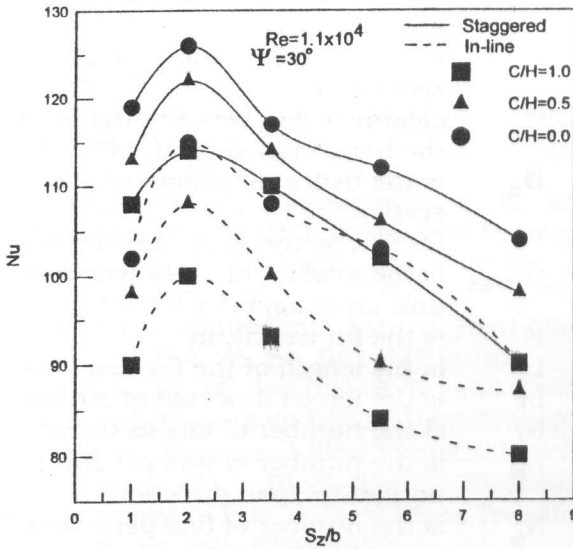


Fig. 11. Comparison of variation of Nusselt number with  $S_z/b$  for in-line and staggered fin arrays ( $S_x=18$  mm,  $\Psi=30^\circ$ , and  $Re = 1.1 \times 10^4$ ).

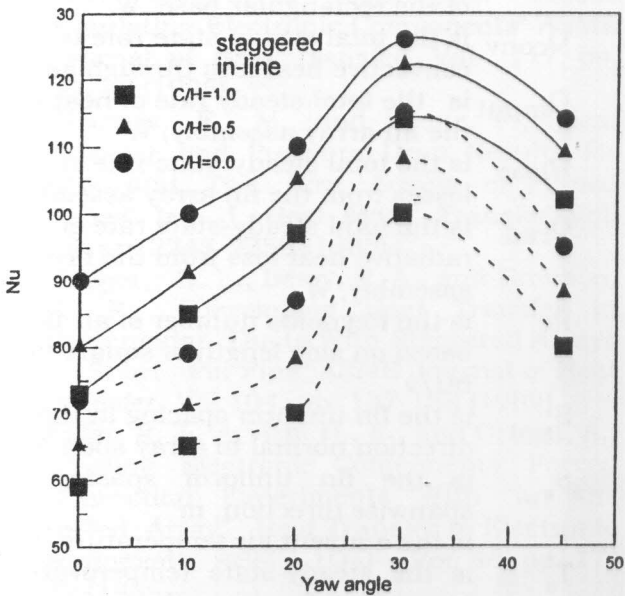


Fig. 12. Comparison of variation of Nusselt number with yaw angle for in-line and staggered fin arrays ( $S_x=18$  mm,  $S_z = 20$ mm, and  $Re=1.1 \times 10^4$ ).

For in-line arrangement:

$$f = 0.54 (Re)^{0.413} (C/H)^{-0.025} (\cos \psi)^{-5.33} (S_x/L)^{-0.44} (S_z/w)^{-0.41}, \quad (14)$$

with spread  $\pm 16\%$ .

For  $C/H=0.0$ ,

$$f = 1.2 (Re)^{-0.494} (\cos \psi)^{-7.1} (S_x/L)^{-0.43} (S_z/w), \quad (15)$$

with spread  $\pm 14\%$ .

For staggered arrangement:

$$f = 0.3 (Re)^{-0.279} (C/H)^{-0.07} (\cos \psi)^{-5.2} (S_x/L)^{-0.41} (S_z/w)^{-0.38}, \quad (16)$$

with spread  $\pm 18\%$ .

For  $C/H=0.0$ ,

$$f = 2.2 (Re)^{-0.5} (\cos \psi)^{-7.6} (S_x/L)^{-0.38} (S_z/w), \quad (17)$$

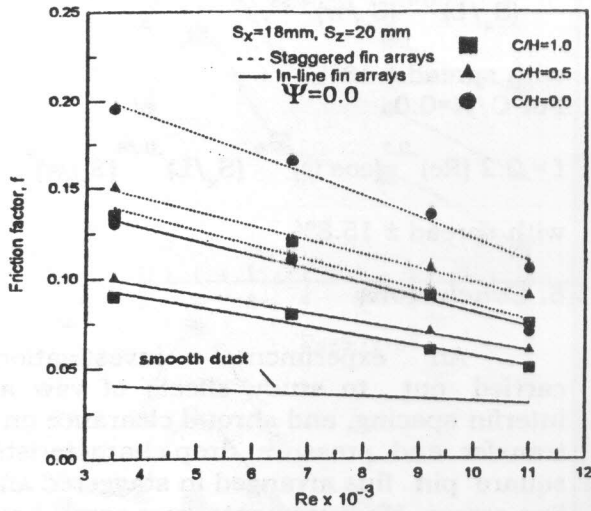
with spread  $\pm 15.8\%$ .

## 5. Conclusions

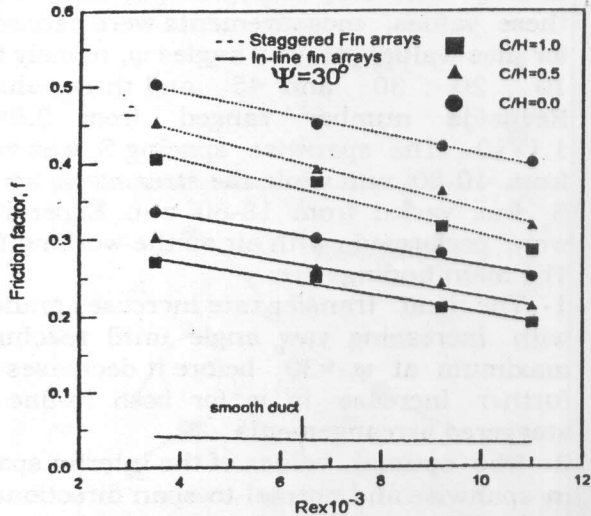
An experimental investigation is carried out to study effects of yaw angle, interfin spacing, and shroud clearance on heat transfer and pressure drop characteristics of square pin fins arranged in staggered and in-line arrays. Measurements were carried out for three values of shroud-to-height ratios  $C/H$ , namely 0.0, 0.5, and 1.0. For each one of these values, measurements were carried out for five values of yaw angles  $\psi$ , namely 0.0, 10, 20, 30 and 45 and three values of Reynolds number ranged from  $3.5 \times 10^3$  -  $1.1 \times 10^4$ . The spanwise spacing  $S_z$  was varied from 10-80 mm while the streamwise spacing  $S_x$  was varied from 18-80 mm. Experiments were performed with air as the working fluid. The main findings are:

- 1- The heat transfer rate increases gradually with increasing yaw angle until reaching a maximum at  $\psi = 30^\circ$  before it decreases with further increase in  $\psi$  for both in-line and staggered arrangements.
- 2- The optimal values of the interfin spacing in spanwise and normal-to-span directions are  $S_z/b = 2.0$  and  $S_x/b = 1.8$  respectively regardless of yaw angle, shroud clearance, and type of array used.
- 3- Staggered arrangement of the array tends to give higher heat transfer rate and higher friction loss than those of the in-line ones regardless of values of shroud clearance-to-height ratio, and yaw angle.

4- General correlations for Nusselt number (Nu) and friction factor (f) have been developed. These correlations take into account normal-to-span spacing  $S_x$ , spanwise spacing  $S_z$ , yaw angle  $\psi$ , shroud-to-height ratio  $C/H$ , and flow Reynolds number  $Re$ , for both in-line and staggered arrangements.



(a)



(b)

Fig. 13. Variation of friction factor  $f$  with Reynolds number  $Re$  at different values of  $C/H$  [ $S_x=18\text{mm}$ ,  $S_z=20\text{mm}$ , (a)  $\psi=0.0$ , (b)  $\psi=30^\circ$ ].

**Nomenclature**

$A_b$  is the fin array total heat transfer area,  $m^2$

- $A_{ff}$  is the free-flow area =  $(C+H) W - N_{fz} b H$ ,  $m^2$
- $b$  is the side length of pin fin cross section,  $m$
- $C$  clearance gap between the fin tip and the horizontal shroud,  $m$
- $D_e$  is the hydraulic diameter of test section,  $m$
- $f$  friction factor,  $[(-\Delta p / \Delta X) \cdot D_e] / (\rho \cdot U^2 / 2)$
- $G_{max}$  is the maximum mass flow rate per unit area,  $kg/m^2 \cdot s$
- $H$  is the fin height,  $m$
- $L$  is the length of the fin assembly,  $m$
- $m$  is the forced flow rate of air,  $kg/s$
- $N_f$  is the number of fins in the assembly
- $N_{fx}$  is the number of fins per row in the normal-to-span direction
- $N_{fz}$  is the number of fins per row in the spanwise direction
- $p$  is the static pressure,  $Nm^{-2}$
- $Pr$  is the Prandtl number,  $C_p \mu / k$
- $Q_a$  is the conductive heat loss from sides of the rectangular base,  $W$
- $Q_{conv}$  is the total steady-state rate of convective heat loss through air,  $W$
- $Q_{input}$  is the total steady rate of heat input to the fin array assembly,  $W$
- $Q_{loss}$  is the total steady-state rate of heat losses from the fin array assembly,  $W$
- $Q_{rad}$  is the total steady-state rate of radiative heat loss from the fin assembly,  $W$
- $Re$  is the Reynolds number of air flow based on side length of square fin,  $bU/v$
- $S_x$  is the fin uniform spacing in the direction normal to array span,  $m$
- $S_z$  is the fin uniform spacing in the spanwise direction,  $m$
- $T_a$  is the ambient air temperature,  $K$
- $T_b$  is the steady-state temperature of the base of pin fin array,  $K$
- $T_{in}$  is the inlet temperature of forced air stream to the pin fin array,  $K$
- $T_{out}$  is the outlet temperature from pin fin array,  $K$
- $t$  is the thickness of base of pin fin array,  $m$
- $U$  is the mean stream velocity,  $m/s$
- $W$  is the width of wind tunnel duct,  $m$
- $w$  is the width of base fin array,  $m$
- $x$  is the normal-to-span direction
- $y$  is the vertical direction

z is the spanwise direction  
 $\psi$  is the yaw angle, deg., (angle between flow direction and normal-to-span direction).

### References

- [1] Sparrow, E. M., Niethammer, J. E., and Chaboki, A., "Heat Transfer and Pressure Drop Characteristics of Arrays of Rectangular Modules Encountered in Electronic equipment" *Int. J. Heat Mass Transfer*, Vol. 25, pp. 961-973 (1982).
- [2] Sparrow, E. M., Vemuri, S. B., and Kadle, D. S., "Enhanced and Local Heat Transfer, Pressure Drop, and Flow Visualization for Arrays of Block-like Electronic Components" *Int. J. Heat Mass Transfer*, Vol. 26, pp. 686-699 (1983).
- [3] Molki, M., Faghri, M., and Ozbay, O., "A Correlation for Heat Transfer and Wake Effect in the Entrance Region of an In-Line Array of Rectangular Blocks Simulating Electronic Components" *ASME Journal of Heat Transfer*, Vol. 117, pp. 40-46 (1995).
- [4] Sparrow, E. M., and Samie, F., "Heat Transfer and Pressure Drop Results for One and Two Row Arrays of Finned Tubes" *Int. J. Heat Mass Transfer*, Vol. 28, pp. 2247-2259 (1985).
- [5] Metzger, D. E., Berry, R. A., and Bronson, J. P., "Developing Heat Transfer in Rectangular Ducts With Staggered Arrays of Short Pin Fins" *ASME Journal of Heat Transfer*, Vol. 104, pp. 137-158 (1989).
- [6] Moffat, R. J., Arvizu, D., E., and Ortega, A., "Cooling Electronic Components: Forced Convection Experiments With an Air-cooled Array" *Heat Transfer in Electronic equipment*, ASME HTD- Vol. 48, pp. 17-27 (1985).
- [7] Moffat, R. J., and Anderson, A. M. "Applying Heat Transfer coefficient Data to Electronic Cooling" presented at the ASME Winter Annual Meeting, Chicago, IL (1988).
- [8] Anderson, A. M., and Moffat, R. J., "A New Type of Heat Transfer Creation for Air Cooling of Rectangular Arrays of Electronic Components" *Proceedings of ASME Winter Annual*, pp. 27-39 (1990).
- [9] Peterson, G. P., and Ortega, A., "Thermal control of Electronic equipment" in: *Advances in Heat Transfer*, Vol. 20, pp. 181-305 (1990).
- [10] Sridhar, S., "Heat Transfer and Fluid Flow Behavior in Array of Rectangular Blocks Encountered in Electronic equipment" M. S. Thesis, Department of Mechanical Engineering and Applied Mechanics, University of Rhode, Island (1990).
- [11] Anderson, A. M., and Moffat, R. J., "Direct Air Cooling of Electronic Components: Reducing Component Temperatures By Controlled Thermal Mixing" *ASME Journal of Heat Transfer*, Vol. 113, pp. 56-62 (1991).
- [12] Faghri, M., Ray, A., and Sridhar, S., "Enhance Heat Transfer Correlation for Air Cooling of Arrays of Rectangular Blocks" *Heat Transfer Enhancement in Electronic Cooling*, ASME HTD-Vol. 183, pp. 19-23 (1991).
- [13] Kang, S. S., "The Thermal Wake Function for Rectangular Electronic Modules" *Proc. National Heat Transfer Conference*, Open Forum, San diago, CA (1992).
- [14] Wirtz, R. A., and Chen, W., "Laminar-Transition Convection From Repeated Ribs in a Channel" *Heat Transfer in Electronic equipment*, ASME HTD-Vol. 171, pp. 89-94 (1991).
- [15] Bejan, A., and Sciubba, E., "The Optimal Spacing of Parallel Plates Cooled by Forced Convection" *Int. Journal of Heat and Mass Transfer*, Vol. 35, pp. 3259-3264 (1992).
- [16] Chu, R. C., and Simons, R. E., "Cooling Technology for High Performance Computers: IBM Sponsored University Research," in: S. Kakac, H. Yuncu, and Hijikata, K., eds., *Cooling of Electronic Systems*, Kluwer Academic Publishers, Dordrecht, The Netherlands, pp. 97-122 (1994).
- [17] Kamath, V., "Air Injection and Convection Cooling of Multi-Chip Modules: A Computational Study" *Proc. InterSociety Conference on Thermal Phenomena in Electronic Systems (ITHERM IV)*, Washington, DC, May 4-7, pp. 83-90 (1994).
- [18] Larson, E. D., and Sparrow, E. M., 1982, "Performance Comparisons Among

- Geometrically Different Pin-Fin Arrays Situated in an Oncoming Longitudinal Flow" *Int. J. of Heat and Mass Transfer*, Vol. 25, pp. 723-725 (1982).
- [19] Mansuria, M. S., and Kamath, V., " Design of Optimization of a High Performance Heat-Sink/Fan Assembly" *ASME HTD-Vol. 292*, pp. 95-103 (1994).
- [20] Matsushima, H., Yanagida, T., and Kondo, Y., " Algorithm for Predicting the Thermal Resistance of Finned LSI Packages Mounted on a Circuit Board" *Heat Transfer Japanese Research*, Vol. 21(5), pp. 504-517 (1992).
- [21] Nakayama, W., Matsushima, H., and Goel, P., "Forced Convection Heat Transfer From Arrays Of Finned Packages" in: *Cooling Technology for Electronic equipment*, W. Aung, ed., Hemisphere, New York, pp. 195-210 (1988).
- [22] Sparrow, E. M., and Larson, E. D., " Heat Transfer From Pin-Fins Situated in an Oncoming Longitudinal Flow Which Turns to Crossflow" *Int. J. of Heat and Mass Transfer*, Vol.25, pp. 603-614 (1982).
- [23] Sathe, S., Kelkar, K. M., Karki, K. C., Lamb, C., and Patankar, S. V., "Numerical Prediction of Flow and Heat Transfer in an Impingement Heat Sink" *ASME EEP-Vol. 4-2*, pp. 893-898 (1983).
- [24] Ledezma, G., Morega A. M., and Bejan, A., "Optimal Spacing Between Pin Fins with Impinging Flow" *Journal of Heat Transfer*, Vol. 118, pp. 570-577 (1996).
- [25] Sullivan, P. F., Ramadhyani, S., and Incropera, F. P., " Extended Surfaces to Enhance Impingement Cooling With Single Circular Liquid Jets" *Advances in Electronic Packages*, ASME, New York, pp. 207-215 (1992).
- [26] Heindel, T. J, Ramaadhyani, S., Incropera, F. P., and Campo, A., " Surface Enhancement of a Heat Transfer Exposed to a Circular Liquid Jet With Annular Collection of the Spent Fluid" *ASME HTD-Vol. 206(2)*, pp. 11-118 (1992).
- [27] Tahat, M. A., "Thermal Optimization of Pin Fin Arrays Experiencing Forced Convection Heat Transfer" M. Sc. Thesis, Cranfield Institute of Technology (1988).
- [28] Jubran, B. A., Hamdan, M. A., and Abdualh R. M., "Enhanced Heat Transfer, Missing Pin, and Optimization for Cylindrical Pin Fin Arrays" *Journal of Heat Transfer*, Vol. 115, pp. 576-583 (1993).
- [29] Kline, S. J., and McClintock, F. A., "Describing Uncertainties on Single Sample Experiments" *Mechanical Engineering*, Vol. 75, pp. 3-8 (1953).
- [30] Naik, S., Probert, S. D., and Shilston, M. J., "Forced Convective Steady State Heat Transfer From Shrouded Vertical Fin Arrays, Aligned Parallel to an Undisturbed Air Stream" *Applied Energy*, Vol. 26, pp. 137-158 (1987).

Received January 15, 2001

Accepted May 6, 2001